Density-functional theory of flux-lattice melting in high-T_c superconductors

Gautam I. Menon*
Department of Physics, Indian Institute of Science, Bangalore-560 012, India

C. Dasgupta,† H. R. Krishnamurthy,† and T. V. Ramakrishnan†
Department of Physics, Indian Institute of Science, Bangalore-560 012, India

Surajit Sengupta
Materials Science Division, Indira Gandhi Centre for Atomic Research, Kalpakkam-603 102, India
(Received 30 April 1996)

Flux-lattice melting in the mixed phase of anisotropic, layered superconductors is studied in the limit of infinite anisotropy. In this limit, if the external field is applied perpendicular to the layer plane, the problem reduces to that of the liquid-solid transition of an assembly of point vortices restricted to move on the superconducting layers and interacting through an anisotropic pair potential. We generalize approximate theories for correlations in the liquid-state to deal with the layering and study the melting of the vortex system using density-functional theory. Calculations of correlation functions measurable in neutron scattering are presented. The theory predicts a first-order melting transition. It has no adjustible parameters and the results are in good agreement with experiments on $Bi_2Sr_2CaCu_2O_8$. [S0163-1829(96)05038-2]

I. INTRODUCTION

When a sample of a type-II superconductor is cooled below its mean-field superconducting transition temperature $T_c(H)$ in an external magnetic field H ($H>H_{c1}$), this field enters the sample in the form of vortex or flux lines. A quantum of flux Φ_0 ($=hc/2e$) is associated with each flux line, while the line itself consists of a central normal core of radial dimension of order of the coherence length ξ, surrounded by circulating supercurrents out to a distance of order λ, the penetration depth, over which the field decays to zero. These flux lines repel each other, stabilizing a triangular lattice of line vortices, which is called a vortex lattice or flux lattice.[1]

Interest in the properties of flux lattices in the context of high-T_c superconductors[2] was first stimulated by early experiments[3–5] which indicated that this lattice underwent a relatively sharp phase transition at temperatures well below $T_c(H)$ in the layered cuprates. While several mechanisms for this transition have been proposed (a rapid crossover from flux creep to flux flow,[6] a spin-glass type of ordering in the presence of weak quenched disorder,[7,8] and glassy states arising out of line entanglement[9]), it is now generally believed that the transition in the pure system is a thermodynamic phase transition in which the flux lattice melts to a liquid of flux lines. This melting transition has been shown to be first order in very pure single-crystal samples of the high-T_c cuprates.[10,11] Such melting transitions are also expected (and have been seen[12]) in low-temperature superconductors close to the upper critical field $H_{c2}(T)$.

We present in this paper a first-principles theory of the melting of the flux lattice (or, equivalently, freezing of the flux liquid) in an anisotropic, layered superconductor as the field or the temperature is varied. This paper represents an elaboration and detailed extension of work published earlier.[13] For concreteness, we study the melting transition in the layered superconductor $Bi_2Sr_2CaCu_2O_8$ (BSCCO) in an external field applied perpendicular to the layer plane. Our theory predicts a weak first-order freezing transition in which the Fourier components of the periodic density field (the order parameters of the solid) change discontinuously across the transition boundary. The only parameters that enter the theory are material parameters, such as ξ, λ, and d, the interlayer spacing for a layered superconductor. We choose as our starting point the limit of infinite anisotropy, i.e., $\gamma=\sqrt{M_c/M_{ab}}\to\infty$, where M_c and M_{ab} are the effective masses of the Cooper pairs perpendicular to and in the plane of the layers. In this limit, if the external magnetic field is applied perpendicular to the layers ($H\|c$), the interaction between flux lines can be rewritten as a sum of pairwise intervortex interactions, where the vortices ''live'' on stacked superconducting layers separated by a distance d. The assumption of infinite anisotropy is equivalent to assuming that the superconducting layers are electronically decoupled or that the contribution to the flux-line energy arising out of the interlayer Josephson coupling is zero.[14] Such an assumption is quantitatively accurate in describing the physics of flux lines in $Bi_2Sr_2CaCu_2O_8$, where γ^2 is believed to exceed 300 (600 in some recent experiments[15]). In this approximation, the flux-line system continues to have a nonzero tilt modulus, as the *electromagnetic* interaction between vortices on different layers is retained. The physical picture is then that of a system of ''pancake'' vortices confined to move on superconducting layers and interacting through an anisotropic pair potential.

We treat this system of vortices as a classical, anisotropic liquid and calculate its correlation functions. There are several advantages to this way of approaching the problem of flux-lattice melting. The system of interacting, directed lines is replaced by a simpler system, that of interacting point vortices. This system of vortices can be treated by well-known methods of classical liquid-state theory. Correlation functions calculated in the liquid phase can be used as input

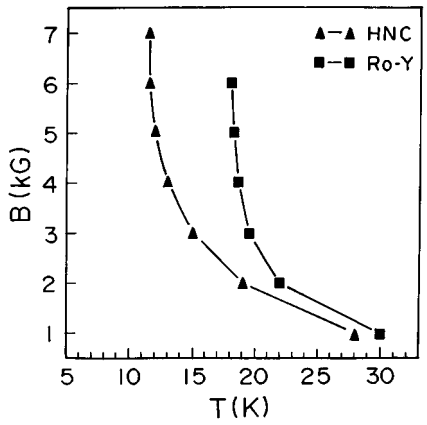

FIG. 1. Liquid-solid phase boundary of $Bi_2Sr_2CaCu_2O_8$ in the *B-T* plane obtained in a density functional theory. Correlations in the flux liquid are calculated in the HNC approximation (triangles) and the Rogers-Young approximation (squares) (see text).

to a density-functional theory of freezing in which the grand-canonical free-energy cost of setting up a static density modulation representing the periodic crystal is computed. The liquid freezes when the free energy of the modulated liquid drops below the free energy of the isotropic liquid. The correlation functions we compute within our theory, which can be related to the equal-time, two-point correlation functions of the magnetic induction within the sample, are experimentally measurable.

Our principal results are summarized in the phase diagram of Fig. 1, where the two types of symbols (solid squares and triangles) show the melting line as calculated in two different approximations (to be explained in the text). For comparison, data taken from three independent experiments on the melting line in BSCCO (redrawn from Refs. 17, 20 and 23), which use pure single crystals with the external field applied perpendicular to the layers, is shown in Fig. 2. Note two qualitative features of the experimental data: (a) The high-field transition temperature is almost independent of field and has an asymptotic value of about 25 K and (b) the transition temperature at low fields is strongly field dependent

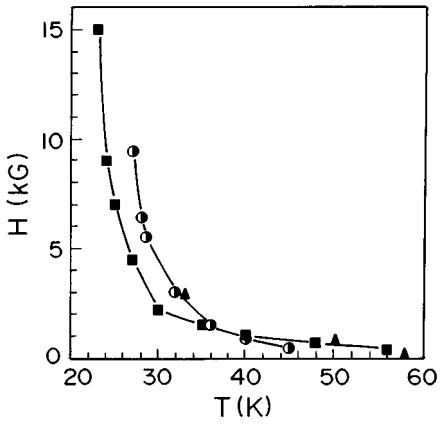

FIG. 2. Experimentally obtained flux-lattice melting phase boundary of $Bi_2Sr_2CaCu_2O_8$ in the *H-T* plane. Redrawn from Ref. 17 (circles), 20 (squares), and 23 (triangles).

and the melting line has a prominent and characteristic curvature. Both these features are rendered correctly in our calculation. In quantitative terms, however, the melting line we calculate lies a little below the transition line seen in experiments. We discuss in detail the reasons for this discrepancy and show that it arises due to the approximate nature of the liquid-state methods we use.

We begin with a brief discussion of experimental results on flux-lattice melting in BSCCO. To make a direct comparison with our results easier, we consider only experiments on pure, single crystal samples with the applied field parallel to the *c* axis.[16] In high-*Q* mechanical oscillator experiments on BSCCO (Refs. 17 and 18) peaks in dissipative response as *H* or *T* is changed are interpreted as signaling phase transitions in the flux-line ensemble.[19] In experiments by Schilling *et al.*, the ''irreversibility line'' (which separates a magnetically irreversible, zero-resistance state from a reversible state with dissipative electrical transport properties) is identified with the melting line.[20,21] These measurements can identify the irreversibility line in BSCCO over several orders of magnitude in field strength and the phase boundary obtained in this manner shares many common features with the melting phase boundary obtained in other experiments. The results of Schilling *et al.* also suggest a crossover between predominantly three-dimensional and two-dimensional fluctuation behavior at the transition as the field is increased. Direct evidence for a flux-lattice melting transition in the mixed phase has come from recent small-angle neutron scattering (SANS) measurements by Cubbitt *et al.*,[22] in which sharp Bragg peaks in the diffracted intensity characteristic of a well-formed triangular lattice are seen to vanish over a narrow temperature range, indicative of a phase transition characterized by a loss of long-range correlations in the spatial distribution of vortex lines. The phase boundary obtained by Cubbitt *et al.* is close to the phase boundary obtained by Lee *et al.*[23] in muon-spin-rotation experiments, where abrupt changes in the space-averaged local-field distribution and its moments as field and temperature are varied, are associated with changes in the flux-line structure at the melting transition. In a very striking recent experiment by Zeldov *et al.*[11] who use a sensitive arrangement of Hall probes to measure the local magnetic induction, a first-order jump discontinuity of the induction is tracked at low fields. This discontinuity vanishes at somewhat larger field values, possibly signaling the increased relevance of disorder at these field values. The experiment of Zeldov *et al.* is particularly significant in that the experimental signatures appear to constitute the first unambiguous demonstration of a first-order flux-lattice melting transition for pure samples, in the high-T_c cuprates.[24]

Theories of flux lattice melting have approached the problem in several ways. Several workers[25–27] have calculated the Lindemann parameter

$$c_L = \sqrt{\langle u^2 \rangle}/a, \tag{1.1}$$

where $\langle u^2 \rangle$ is the mean square thermal fluctuation in the flux-line positions and a is the mean interline spacing, typically within a harmonic approximation for the solid. According to the Lindemann criterion, the lattice melts when c_L becomes larger than a value c_M, with c_M being approximately universal in simple, three-dimensional solids. Hough-

ton, Pelcovits, and Sudbø[25] use the wave-vector-dependent elastic constants of the vortex system to calculate $\langle u^2 \rangle$ but extract unusually large Lindemann parameters in their fits to experimental data ($0.3 < c_M < 0.4$), in comparison to values obtained in simple, relatively isotropic, three-dimensional solids where c_M is smaller by a factor of 4. Although the Lindemann criterion is often a good indicator of melting in three dimensions, it is necessary to emphasize here that it is by no means a *theory* of the melting transition, the value of c_M being essentially *ad hoc*. In work by Glyde, Moleko, and Findeisen,[28] a self-consistent phonon theory is used to infer the boundary in the B-T plane across which a lattice instability sets in. The phase boundary they calculate, however, has far more curvature at high fields than the experimental data and also lies systematically below it.[29]

In work by Nelson and Seung,[30] the analogy of the partition function of the flux-line system with the path-integral representation of a system of two-dimensional, interacting bosons is used to infer the nature of the melting transition using the known behavior of the boson model. Boson trajectories in $2+1$ dimensions are identified with flux lines (with the time direction for the boson problem being identified with the direction of the external field for flux lines), and these bosons interact through an interaction which is local in time; i.e., the interaction between flux lines operates in a constant z slice. The approximations of Nelson and Seung should be accurate as $B \rightarrow 0^+$, and their theory predicts the existence of a sliver of reentrant liquid at sufficiently low fields. At higher field values, however, the approximation that the bosons interact locally in time should break down.[31] A theory of the flux-lattice melting transition in two dimensions has also been proposed by Herbut and Tesanovic using the observation that the partition function of the vortex system in the ''lowest Landau level approximation'' is equivalent to that of a classical two-dimensional plasma with many-body (gauge) interactions.[32]

Other models for the transition in the layered cuprates include dislocation-mediated melting models for independent melting transitions within each layer.[33,34] However, such theories fail to take into account the three-dimensional (long-ranged) electromagnetic interaction between vortices on different layers, which, although weak, must always be present. It is only asymptotically in the limit of very large fields that the vortex system becomes two dimensional — as we have shown earlier,[13] transverse (c-axis) correlation lengths are bounded below by lengths of order of five to six interlayer spacings for typical laboratory fields, indicating that the three-dimensional nature of the interactions cannot be neglected.

Ryu *et al.*,[35] in Monte Carlo simulations of a model for interacting flux lines in anisotropic superconductors, argue for the existence of distinct flux-liquid and flux-solid phases separated by a phase boundary that shares many common features with the experimental data. They determine this boundary by monitoring crystalline order as manifested in the structure factor $S(\vec{q}=\vec{G}_1)$ where G_1 is any of the six reciprocal lattice vectors associated with the first shell in reciprocal space. They find that c_M is not constant along the whole phase boundary but changes from a value of about 0.4 at very high fields to about 0.16 at low fields, with c_M being fixed at about 0.2 for much of the intermediate-field region. As in this paper, their basic interaction is a two-point interaction between point vortices that move on superconducting planes, but Ryu *et al.* also allow point vortices which belong to the same vortex line but which are separated by a layer to interact through a Josephson interaction. The form of the intervortex interaction they use is, however, an approximation to the actual interaction between vortex lines and does not include the electromagnetic interaction between pancake vortices. Hetzel, Sudbø, and Huse,[36] in a Monte Carlo simulation of a three-dimensional, anisotropic, uniformly frustrated XY model (a latticized version of the anisotropic Ginzburg-Landau model where amplitude fluctuations as well as gauge-field fluctuations are neglected), find clear evidence for a first-order transition, with an entropy change on melting of about $0.3k_B$ per vortex per layer.[37] Recent detailed Monte Carlo simulations by Sasik and Stroud,[38] which allow the magnetic induction to assume different values in the solid and liquid phases, see unambiguous evidence for a first-order flux-lattice melting transition using parameter values appropriate to $YBa_2Cu_3O_{7-\delta}$ (YBCO). In their work, the transition manifests itself as a discontinuity in the magnetization. In addition, their calculated structure factors show Bragg peaks characteristic of triangular ordering in the solid phase, vanishing to yield liquidlike rings as they scan across a temperature interval of about 0.3 K at the transition boundary.

The approach to the flux-lattice melting problem discussed in this paper differs from other approaches in several distinct and fundamental ways. Our calculation is a first-principles calculation in that the only inputs to the theory are material parameters which can be obtained through independent measurements on the system. The mapping of the flux-line system to a system of point vortices which interact through a pairwise interaction is a controlled starting point for our theory which then uses traditional liquid-state methods to calculate the correlation functions of the flux-liquid phase. The density-functional approach to the liquid-solid transition enables us to use these correlation functions to accurately compute the liquid-solid boundary. Our calculation differs from Lindemann-parameter-based theories in that the Lindeman parameter is a calculable quantity within the framework of our theory and not a free parameter. Our calculation also spans the entire regime of field and temperature values (provided fluctuations in the amplitude of the pair-wave function can be neglected and quantum effects are small), unlike theories based on the boson mapping, or the lowest Landau level approximation. Our model works with the full screened interaction, unlike the lattice models proposed by Hetzel *et al.* and by Li and Teitel.[39] Also, our calculations, unlike the simulations, do not suffer from statistical errors.

The outline of this paper is as follows. In Sec. II, we briefly review the mapping of the vortex-line Hamiltonian to one involving pairwise interactions between point vortices in the limit of infinite anisotropy. We then discuss liquid-state methods for the calculation of correlation functions in the liquid-state and motivate the use of density-functional theory in the prediction of the liquid-solid phase boundary. In Sec. III, we discuss in detail our results in the hypernetted-chain (HNC) approximation. We point out the need for going beyond the HNC approximation to obtain the freezing line ac-

curately. An improved liquid-state theory for the flux liquid, an extension of an approximation suggested by Rogers and Young[40] for the two-dimensional one-component plasma, is presented in Sec. IV. In Sec. V we extract correlation functions of the vortex system which are measurable in neutron scattering and in muon-spin-rotation experiments. Finally, in Sec. VI, we comment on our results in the light of experiments on anisotropic superconductors such as BSCCO, and point out possible extensions of our theory.

II. BASIC FORMALISM: LIQUID STATE AND DENSITY- FUNCTIONAL METHODS

Many of the characteristic features of flux arrays in high-T_c superconductors can be understood as arising out of properties such as short coherence lengths, elevated transition temperatures, intrinsic layering, large penetration depths, and the existence of considerable anisotropy in physical properties between directions along and perpendicular to the layering direction. These features combine to increase the effects of thermal fluctuations in the mixed state. If the c-axis coherence length (ξ_c) is of order the interlayer spacing d (a condition satisfied by BSCCO for temperatures $T<0.99T_c$), it is necessary to incorporate the layering from the outset, in a free-energy functional first suggested by Lawrence and Doniach.[41] The Lawrence-Doniach functional appropriate for the anisotropic high-T_c cuprates takes the form[34,41]

$$F=F^0+F^J, \tag{2.1}$$

where

$$F^0=d\sum_n \int d^2\rho\left[\alpha|\Psi_n(\vec{\rho})|^2+\frac{\beta}{2}|\Psi_n(\vec{\rho})|^4+\frac{1}{2M^\star_{ab}}\left|\times\left(-i\hbar\vec{\nabla}_\rho-2\frac{e}{c}\vec{A}_\rho\right)\Psi_n\right|^2\right]+\int d^3r\frac{|\vec{\nabla}\times\vec{A}(\vec{r})|^2}{8\pi} \tag{2.2}$$

and

$$F^J=\sum_n \int d^2\rho\,\frac{\hbar^2}{2M^\star_c d}\left|\Psi_{n+1}(\vec{\rho})\exp\left(\frac{i2e}{\hbar c}\int_{-\infty}^{(n+1)d}\vec{A}\cdot\vec{dl}\right)-\Psi_n(\vec{\rho})\exp\left(\frac{i2e}{\hbar c}\int_{-\infty}^{nd}\vec{A}\cdot\vec{dl}\right)\right|^2. \tag{2.3}$$

Equations (2.1)–(2.3) represent the free energy of a set of superconducting planes (with coordinates given by n, the layer index, and ρ, the radial in-plane distance), coupled through a Josephson interaction. Here d is the interlayer spacing, $M^\star_{ab}$ represents the in-plane (a-b plane) effective mass, $M^\star_c$ the c-axis effective mass, and $\vec{A}(\vec{r})$ is the magnetic vector potential. The parameters α and β are phenomenological parameters with $\alpha\propto(T-T_c)$ and β approximately constant close to T_c. Transforming to phase variables using $\Psi=\Psi_0(\mathbf{r})\exp[i\theta(\mathbf{r})]$, and assuming that the *magnitude* of the order parameter is constant everywhere except at the core of a vortex, the following phase functional can be derived:

$$E[\theta_n]=\frac{J}{2}\sum_n \int d^2\rho\left\{\left|\vec{\nabla}_\rho\theta_n-\frac{2e\vec{A}_\rho}{\hbar c}\right|^2+\frac{2}{\lambda_J^2}\left[1-\cos\left(\theta_{n+1}-\theta_n-\frac{2\pi}{\Phi_0}\int_{nd}^{(n+1)d}A_z dz\right)\right]\right\}+\int d^3r\frac{[\vec{\nabla}\times\vec{A}(\mathbf{r})]^2}{8\pi}. \tag{2.4}$$

Here $J/2$ is $\Phi_0^2 d/32\pi^3\lambda_{ab}^2$ and λ_J is $\lambda_c d/\lambda_{ab}$ where the London penetration depths λ_i are defined by $\lambda_i^2=M_i^\star c^2/4\pi(2e)^2\Psi_0^2$, with $M_i^\star=M^\star_{ab},M^\star_c$.

Assuming infinite anisotropy, i.e., $M^\star_c\to\infty$, the distribution of fields and of the phase in the layered superconductor is given by the London equation,

$$-\nabla^2\mathbf{A}=\frac{\Phi_0 d}{2\pi\lambda_{ab}^2}\sum_n\left(\vec{\nabla}_\rho\theta-\frac{2e\vec{A}}{\hbar c}\right)\delta(z-nd), \tag{2.5}$$

which must be supplemented by the relation

$$\vec{\nabla}_\rho\times\vec{\nabla}_\rho\theta_n=2\pi\hat{n}_z\sum_k \delta(\vec{\rho}-\vec{\rho}_{n,k}). \tag{2.6}$$

We have assumed that the vorticities are nonzero only on the layers, that they are oriented in the c-axis direction given by the unit vector $\hat{n}_z$, and that the locations of the vortices on the nth layer are given by $\vec{\rho}_{n,k}$. (We also set $\lambda=\lambda_{ab}$ for ease of notation.) Additionally, it can be assumed that the field varies sufficiently slowly across the layers ($\lambda\gg d$) so that we can replace $\vec{A}(\vec{\rho},nd)$ by $\vec{A}(\vec{r})$.

In this limit of infinite anisotropy, the interaction energy of a set of planar vortices can now be derived from the solutions to Eqs. (2.5) and (2.6) which minimize Eq. (2.4).[34,42] The pairwise form of this interaction follows from the quadratic nature of the effective phase functional in this limit. In Fourier space, the intervortex interaction reads

$$\beta V(\mathbf{k})=\frac{\Gamma\lambda^2[k_\perp^2+(4/d^2)\sin^2(k_z d/2)]}{k_\perp^2[1+\lambda^2k_\perp^2+4(\lambda^2/d^2)\sin^2(k_z d/2)]}, \tag{2.7}$$

with $\Gamma=\beta d\Phi_0^2/4\pi\lambda^2$ and $\beta=1/k_BT$. The wave vector $k_\perp$ refers to the in-plane coordinates and k_z to the out-of-plane (z direction) coordinate.

This expression can be rewritten as

$$\beta V(\mathbf{k}_\perp,k_z)=\frac{\Gamma}{k_\perp^2}\left[1-\frac{1}{(1+\lambda^2\tilde{k}_z^{\,2})}\right]+\frac{\Gamma\lambda^2}{(1+\lambda^2\tilde{k}_z^{\,2})(1+\lambda^2k_\perp^2+\lambda^2\tilde{k}_z^{\,2})}, \tag{2.8}$$

with $\tilde{k}_z^{\,2}=4/d^2\sin^2(k_z d/2)$. The asymptotic ($\rho\to\infty$) properties of the real space interaction follow from the Fourier transform of the first term in Eq. (2.8). At large distances with $n=0$, the interaction is repulsive and is of the form

$$V(\rho,n=0)\sim-\frac{\Gamma}{2\pi}\ln\left(\frac{\rho}{L}\right), \tag{2.9}$$

where L is an arbitrary scaling length and ρ denotes the in-plane separation.

The interaction between vortices separated by a layer or more is attractive, favoring the formation of vortex lines at sufficiently low temperatures. For large ρ, the interaction is supressed by a factor of λ/d, i.e.,

$$V(\rho,n\neq 0)\sim -\left(\frac{d}{\lambda}\right)\exp(-nd/\lambda)\times V(\rho,n=0). \tag{2.10}$$

As a consequence, the interlayer interaction is always weaker than the intralayer interaction. If $\lambda=1500$ Å and $d=15$ Å (reasonable values for BSCCO), this implies that interlayer interactions are weaker by a factor of 100. This observation will be of use in motivating an ansatz for the asymptotic behavior of liquid-state correlation functions involving vortices on different layers.

Given this potential of interaction between vortices, the evaluation of equal-time correlation functions in the vortex liquid can be reduced to a problem in classical liquid-state theory.[43] The basic quantities calculated are the pair distribution function $g(|\mathbf{r}-\mathbf{r}'|)$, defined by $\langle\Sigma_{i=1}^{N}\Sigma_{j\neq i}^{N}\delta(\mathbf{r}-\mathbf{r_i})\,\delta(\mathbf{r}'-\mathbf{r_j})/\rho_{\ell}^{2}\rangle$, the pair correlation function $h(r)$ defined by $h(r)=g(r)-1$, and the static structure factor defined by

$$S(q)=1+\rho_{\ell}\int d^{d}r\,h(r)\exp(i\mathbf{q}\cdot\mathbf{r}).$$

Here ρ_{ℓ} is the density of the liquid. The pair correlation function for a simple, isotropic fluid can be decomposed as

$$h(r)=C(r)+\rho_{\ell}\int d^{d}r'\,C(|\mathbf{r}-\mathbf{r}'|)h(\mathbf{r}'), \tag{2.11}$$

which is the Ornstein-Zernike relation.[43] This convolution relation replaces the long-ranged function $h(r)$ by the shorter-ranged $C(r)$ (termed the direct correlation function) which can be related to the structure factor through $S(q)=1/[1-\rho_{\ell}C(q)]$. Translational invariance for a three-dimensional simple liquid implies that these correlation functions are functions of the radial coordinate only. For the vortex system, these correlation functions will be functions of the separation in cylindrical coordinates ρ as well as of the layer separation n.

To supplement the Ornstein-Zernike relation, a closure relation is needed between $h(r)$ and $C(r)$. Such a relation can be derived perturbatively[43] and is of the form

$$C(r)=\exp[-\beta V(r)+Y(r)+B(r)]-1-Y(r), \tag{2.12}$$

where $V(r)$ is the interparticle pair potential, $Y(r)=h(r)-C(r)$, and $B(r)$, the so-called bridge function, represents the sum over a particular infinite set of diagrams in the perturbation expansion. No closed expression is available for the bridge function in general, and it is necessary to approximate it in some way. In the hypernetted-chain or (HNC) closure, the bridge function is set to zero to yield

$$C(r)=\exp[-\beta V(r)+Y(r)]-1-Y(r). \tag{2.13}$$

The self-consistent solution of Eqs. (2.11) and (2.13) constitute the liquid-state theory approach to the calculation of correlations in the liquid-state within the HNC scheme. More elaborate closure schemes exist which improve on the HNC theory, particularly in establishing thermodynamically consistent equations of state. We will discuss one of these schemes in Sec. IV.

In our analysis we use density-functional methods[44–46] to calculate the boundary between the solid and liquid phases of the vortex system. Within density-functional theory, the free energy of an arbitrary time-averaged density configuration is expressed in terms of fluid-phase correlation functions. Freezing into a particular crystal structure occurs when the free energy associated with setting up the appropriate density modulation in the fluid equals the free energy of the uniform liquid. The only inputs to the theory are correlation functions in the liquid-state, which may be obtained either directly from experiment, from simulations, or from liquid-state theories.

In the density-functional theory of Ramakrishnan and Yussouff,[44] the grand-canonical free-energy cost (with respect to the uniform liquid) of producing a time-averaged density inhomogeneity is expressed as a functional of the density $\rho(\mathbf{r})$ (not to be confused with ρ, the radial coordinate defined earlier). The simplest such functional reads

$$\frac{\Delta\Omega}{k_BT}=\int d^{d}r\left[\rho(\mathbf{r})\ln\frac{\rho(\mathbf{r})}{\rho_{\ell}}-\delta\rho(\mathbf{r})\right]-\frac{1}{2}\int d^{d}r\int d^{d}r'\,C^{(2)}\times(|\mathbf{r}-\mathbf{r}'|)[\rho(\mathbf{r})-\rho_{\ell}][\rho(\mathbf{r}')-\rho_{\ell}]\cdots, \tag{2.14}$$

where $\rho(\mathbf{r})$ is the density at point $\mathbf{r}$, $\delta\rho(\mathbf{r})$ is $\rho(\mathbf{r})-\rho_{\ell}$, $C^{(2)}(\mathbf{r},\mathbf{r}')$ $[\equiv C(\mathbf{r},\mathbf{r}')$ as defined earlier] is the pair direct correlation function, T is the temperature, ρ_{ℓ} is the liquid density, and the ellipsis denotes higher-order terms in the correlation functions. In practice, the correlation functions $C^{(n)}(\mathbf{r}_1,\mathbf{r}_2,\ldots\mathbf{r}_n)$, with $n>2$, are difficult to obtain (although they are typically small) and it is conventional to set them to zero.

At the mean-field level, density configurations which represent the equilibrium phase minimize Eq. (2.14), i.e., satisfy $\delta\Delta\Omega/\delta\rho(\mathbf{r})=0$. This minimization condition is easily seen to be

$$\ln\left[\frac{\rho(\mathbf{r})}{\rho_{\ell}}\right]=\int d\mathbf{r}'\,C^{(2)}(|\mathbf{r}-\mathbf{r}'|)[\rho(\mathbf{r}')-\rho_{\ell}]. \tag{2.15}$$

Periodic (crystalline) density configurations which are the solutions of the mean-field equations must therefore satisfy the self-consistency condition

$$1+\eta+\sum_{\mathbf{G}\neq\mathbf{0}}\rho_{\mathbf{G}}\exp(i\mathbf{G}\cdot\mathbf{r})=\exp\left(\widetilde{C}_0^{(2)}\eta+\sum_{\mathbf{G}\neq\mathbf{0}}\widetilde{C}_{\mathbf{G}}^{(2)}\rho_{\mathbf{G}}\times\exp(i\vec{G}\cdot\vec{r})\right), \tag{2.16}$$

where the $\mathbf{G}$'s are the reciprocal lattice vectors of the structure to which the liquid freezes, $\rho_{\mathbf{G}}$'s are the Fourier components of the density field with wave vector $\mathbf{G}$, and we have defined $\widetilde{C}\equiv\rho_{\ell}C$. We have explicitly extracted the $G=0$ component η, which is the fractional volume change on

freezing from the liquid. Note that $\rho_{\mathbf{G}}=0$, for all $\mathbf{G}\neq 0$, is always a minimum of the density functional and represents the uniform liquid. Because of the nonlinearity of the self-consistency condition, however, periodic density-wave solutions which could be absolute minima of Eq. (2.14) may appear suddenly as the correlations increase. The liquid freezes when the free energy of the periodic solid and that of the liquid are equal. In terms of the Fourier components of the density field, the free energy takes the following form

$$\frac{N\Delta\Omega}{k_BT}-\rho_{\diagup}\eta=\frac{1}{v}\int^{\text{cell}}d^dr\left[\left(1+\eta+\sum_{\mathbf{G}\neq\mathbf{0}}\rho_G\exp(i\mathbf{G}\cdot\mathbf{r})\right)\times\left(\widetilde{C}_0^{(2)}\eta+\sum_{\mathbf{G}\neq\mathbf{0}}\widetilde{C}_{\mathbf{G}}^{(2)}\rho_{\mathbf{G}}\exp(i\vec{G}\cdot\vec{r})\right)\right]-\frac{1}{2}\left(\widetilde{C}_0^{(2)}\eta+\sum_{\mathbf{G}\neq\mathbf{0}}\mu_{\mathbf{G}}^2\widetilde{C}_{\mathbf{G}}^{(2)}\right). \tag{2.17}$$

Equation (2.16) is to be solved, in principle, for each member of the infinite set of $\mu_{\mathbf{G}}$'s. This can be done in several ways. First, the equations for each order parameter [$\rho_{G_1},\rho_{G_2},\ldots$ in Eq. (2.16)] can be solved by retaining only a few order parameters and solving Eq. (2.16) in terms of these. This technique has the disadvantage of being numerically cumbersome, especially when $\widetilde{C}^{(2)}(k)$ decays slowly and many order parameters have to be retained to accurately describe the transition. For this reason, variational methods which make an ansatz for the *full* set of ρ_G's (such as assuming the periodic density distribution to be expressible in terms of a sum over Gaussian density profiles centered at the lattice sites, with the width and the amplitude of the Gaussian calculated variationally) are common.[45,46] The variational method, however, suffers from the drawback that the density profile assumed is to an extent arbitrary. In this paper, following Ramakrishnan,[47] who observed that a few (one or two) order parameter theory gives good results for two-dimensional systems, we will use a finite set of order parameters to describe the solid and will examine the behavior of the melting curve as more and more order parameters are included. Additional justification for this approximation comes from the observation that the appropriate input $C^{(2)}(k)$ decays to zero extremely fast for large k, so that the approximation of truncating the full order parameter set is valid.

The crystalline state of the flux-line system maps, in this model, to a three-dimensional lattice of vortices formed by a regular stacking (in registry) of triangular arrays of vortices on each layer. The appropriate density functional is then a functional of a two-dimensional density field with the symmetry of the triangular Abrikosov lattice and the appropriate input is the direct correlation function $C^{(2)}(k_\perp,k_z=0)$. In the following two sections we will descibe calculations of this quantity based on two approximate closure relations, the hypernetted-chain (HNC) approximation and the Rogers-Young approximation. We will demonstrate the need for going beyond the HNC approximation to get reasonable values for the freezing line. As we will show, this is because of an intrinsic deficiency of the HNC approximation: its underestimation of correlations in the liquid-state for this problem.

We end this section by commenting briefly on one possible deficiency of our model for the flux-line system. In the case of flux lines, fluctuations in the flux-line number can strictly occur only through the addition of an infinite number of planar vortices (the number of planar vortices being the same for each layer). However, we have implicitly assumed in our use of results for classical liquids that the vortex numbers can fluctuate arbitrarily from layer to layer, i.e., we work in a grand-canonical ensemble for the vortices with a chemical potential conjugate to the vortex density and not to the density of lines. We do not believe that such a constraint would materially affect our results for correlations except for $k\rightarrow 0$. Corrections to the correlation functions arising from this constraint would, however, be important at sufficiently low fields where the flux-line lattice is highly compressible and the small-k behavior of the correlation functions must be treated accurately.

III. CORRELATION FUNCTIONS IN THE HNC APPROXIMATION

We describe in this section calculations based on a HNC theory of the vortex liquid by making the appropriate generalization to the layered case. We begin by observing that at sufficiently large distances, the asymptotic behavior of the direct correlation function is known to be of the form

$$C(r)\sim-\beta V(r). \tag{3.1}$$

As the interlayer vortex-vortex interaction is weaker than the intralayer interaction by a factor of about 100, we expect correlations between vortices on different layers to be weaker than correlations between vortices on the same layer in general. As a first approximation, then, we can replace the full $C^n(\rho)$, for all $n\neq 0$, by its asymptotic value as given in Eq. (3.1). The generalization of the HNC equation to the layered case reads

$$C^n(\rho)=\exp[-\beta V(\rho,nd)+Y^n(\rho)]-1-Y^n(\rho), \tag{3.2}$$

where the superscript n refers to the layer separation. The Ornstein-Zernike relation, which now involves a convolution over layer index as well, assumes the form (where we have defined our Fourier transforms so as to eliminate factors of the density)

$$C(k_\perp,k_z)=h(k_\perp,k_z)+C(k_\perp,k_z)h(k_\perp,k_z). \tag{3.3}$$

Equations (3.2) and (3.3) form an infinite set of equations which must, in principle, be solved for *each* of the C^n's. To further simplify the calculation we now split the direct correlation function into a short- and a long-ranged part as $C^n(\rho)=C_s^n(\rho)+C_L^n(\rho)$ where we choose $C_L^n(\rho)=-\beta V(\rho,nd)$ as above. In addition, we define $Y^n(\rho)=Y_s^n(\rho)+Y_L^n(\rho)$, with $Y_L^n(\rho)=+\beta V(\rho,nd)$. The assumption that the full direct correlation function $C^n(\rho)$, for all $n\neq 0$, can be represented well by the asymptotic value C_L^n then translates into the ansatz that the short-ranged part of C^n is of the form

$$C_s^n(\rho)=C_s^0(\rho)\,\delta_{n,0}. \tag{3.4}$$

We define our (dimensionless) Fourier transforms as

$$F(\vec{k}_\perp,k_z)=\rho_A\sum_{n=-\infty}^{\infty}\int d^2\rho F(\vec{\rho},nd)\exp(i\vec{k}_\perp\cdot\vec{\rho}+ik_znd) \tag{3.5}$$

and

$$F(\vec{\rho},nd)=\rho_A^{-1}\frac{d}{2\pi}\int_{-\pi/d}^{\pi/d}dk_z\int d^2k_\perp F(\vec{k}_\perp,k_z)$$
$$\times\exp(-i\vec{k}_\perp\cdot\vec{\rho}-ik_znd), \tag{3.6}$$

where ρ_A represents the areal density of vortices. The mean interparticle spacing (MIPS) sets the unit of length such that $\rho_A=1/\pi$. For consistency with this definition of the Fourier transform the intervortex potential [Eq. (2.7)] should be multiplied by an additional factor of $1/\pi$. The HNC equation for the single layer $n=0$ can now be written in terms of the short-ranged part as

$$C_s^0(\rho)=\exp[Y_s^0(\rho)]-1-Y_s^0(\rho), \tag{3.7}$$

where the Fourier space $Y_s^0(k_\perp)$ must satisfy

$$Y_s^0(k_\perp)=\frac{d}{2\pi}\int_{-\pi/d}^{\pi/d}dk_z\frac{C_s^0(k_\perp)+C_L(k_\perp,k_z)}{1-C_s^0(k_\perp)-C_L(k_\perp,k_z)}-C_s^0(k_\perp). \tag{3.8}$$

The problem of solving the infinite set of HNC equations has now reduced to the evaluation of a single function $C_s^0(\rho)$, from the self-consistent solution of Eq. (3.7) and the Ornstein-Zernike (3.8). The quantities being iterated have no long-range tails as these have been explicitly subtracted out. A further simplification can be made in that it is also possible to carry out the k_z integration in Eq. (3.8) analytically. One gets

$$Y_s^0(k_\perp)=\frac{k_\perp^2}{\sqrt{C^2-D^2}}\left(A-\frac{BC}{D}\right)+k_\perp^2\frac{B}{D}-1-C_s^0(k_\perp), \tag{3.9}$$

where

$$A=1+\lambda^2k_\perp^2+2\frac{\lambda^2}{d^2},$$

$$B=-2\frac{\lambda^2}{d^2},$$

$$C=[1-C_s^0(k_\perp)]k_\perp^2\left(1+\lambda^2k_\perp^2+2\frac{\lambda^2}{d^2}\right)+\frac{\Gamma}{\pi}\left(\lambda^2k_\perp^2+2\frac{\lambda^2}{d^2}\right),$$

$$D=-2\frac{\lambda^2}{d^2}\left([1-C_s^0(k_\perp)]k_\perp^2+\frac{\Gamma}{\pi}\right). \tag{3.10}$$

We iterate these equations using a method due to Gillan,[48] which we describe here briefly for completeness. In this method, the function to be iterated over is split into a ''coarse'' and a ''fine'' part, with the coarse part being decomposed in terms of a set of predetermined basis functions. The iteration proceeds in terms of the coefficients of the basis functions, with the fine part being added at each stage of the iterative minimization. The two-dimensional Fourier transforms (actually Hankel transforms because of rotational invariance of the correlation functions in the plane) are evaluated by a quadrature method proposed by Lado.[49] The functions are tabulated at $N_{\max}$ points, with $N_{\max}$ ranging from 700 to 1200. It is necessary to include a cutoff for the Fourier integration procedures. This cutoff is determined by the criterion that the converged functions should be independent of the cutoff used [in practice we have found that cutoffs of the order of 10 (in MIPS units) in real space are sufficient]. The iteration proceeds until convergence to 1 part in 10^8 is achieved between successive iterations.

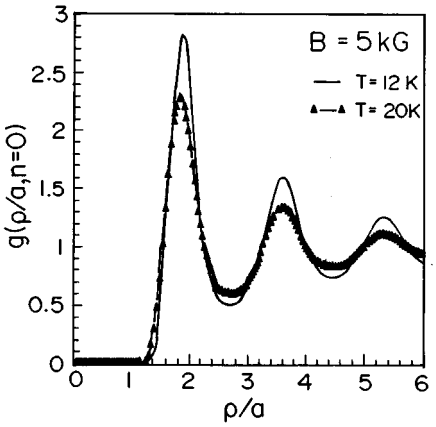

FIG. 3. Pair distribution function $g(\rho,n=0)$ vs ρ calculated in the HNC approximation for parameter values $B=5$ kG and $T=12$ and 20 K. In this and other figures, all lengths are measured in units of the mean interparticle spacing a defined by $\pi a^2\rho_A=1$ where ρ_A is the areal density.

In Fig. 3 we show the pair distribution function $g(\rho,n=0)$ as a function of ρ, calculated in the HNC approximation, for the temperatures $T=12$ and 20 K at a fixed value of the induction $B=5$ kG. Note the considerable structure in $g(\rho,n=0)$ which builds up as the temperature is decreased. In Fig. 4, we show the off-layer pair distribution function $g(\rho,n=1,4,10)$ calculated in the HNC approxima-

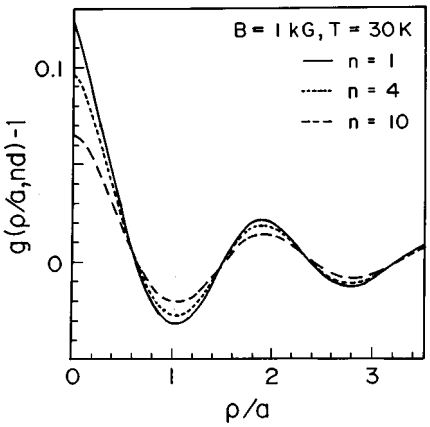

FIG. 4. Off-layer pair distribution function $g(\rho,n)$ vs ρ for $n=1$, 4, 10, calculated in the HNC approximation for parameter values $T=30$ K and $B=1$ kG. The peak at $\rho=0$ indicates correlations arising from the fact that vortices on different layers attract each other.

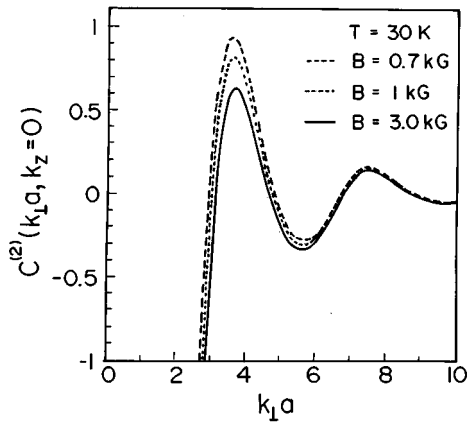

FIG. 5. Results of an HNC calculation of $\tilde{C}^{(2)}(k_\perp, k_z=0)$ vs $k_\perp$ for $T=30$ K and $B=0.7$, 1.0, and 3 kG. Note the increase in structure which occurs as the field is decreased.

tion, at a fixed value of the induction $B=1$ kG and a temperature of 30 K. As n is increased, off-layer correlations decrease as expected; the peak at $\rho=0$ is a consequence of the *attractive* interaction between vortices on different layers. The height of this peak decreases as the temperature is increased (at fixed B) and increases as the field is decreased (at fixed temperature T). In Fig. 5, we show $\tilde{C}^2(k_\perp, k_z=0)$ at $T=30$ K for values of the induction $B=0.7$, 1, and 3 kG. The structure in this correlation function, which is used as input to the freezing calculation, increases rapidly as the field is decreased. This increase drives the transition to the Abrikosov flux lattice at *low* fields or, equivalently, as the density is decreased, and also signals the increase in importance of off-layer correlations. [The field strength is expressed in terms of the magnetic induction B which controls the areal density or vortices through $\rho_A \Phi_0 = B$, rather than the externally applied field H. The distinction, which can be calculated given the constitutive relation $B=B(H)$, is small at typical laboratory fields ~ 1 kG].

We calculate the freezing line by making use of Eq. (2.16) and the free-energy functional (Eq. 2.17), with the input $C^{(2)}(k_\perp, k_z=0)$ taken from the results of the liquid-state calculation. We vary the number of order parameters used in the calculation (from 1 to 6) to check that the approximation of using only the first few order parameters can be justified, and obtain ρ_{G_1}, the order parameter at the smallest nonzero reciprocal lattice vector $G=G_1$, by iterating Eq. (2.16), the self-consistency equation for the order parameters. The effect of including more order parameters gives results indistinguishable from those plotted. This is because $C^{(2)}(k_\perp, k_z)$ in this system decays very rapidly to zero. The order parameter jump at the transition is about 50% of its value at $T=0$.

We calculate the Lindemann parameter using the expression

$$\langle u^2 \rangle = \frac{1}{v} \int^{\text{cell}} d^d r r^2 \frac{\rho(\mathbf{r})}{\rho_\ell}, \tag{3.11}$$

where $\rho(\mathbf{r})$ is the density of the solid at the freezing transition and v is the unit cell volume. We obtain a Lindemann number which is approximately constant and has the value of 0.2 in the field range we consider (0.6 – 10 kG).

Our results for the freezing line in the HNC approximation for liquid-state correlations are plotted in Fig. 1 as the triangles joined by a solid line. The discrepancy between theory and experiment is quantitative rather than qualitative — while the structure of the experimental curve is well reproduced, the calculated melting line lies systematically below the experimentally obtained melting line. In the next section, we turn to another approximation common in the study of liquids, the Rogers-Young approximation.[40] This approximation goes some way towards correcting the systematic underestimation of liquid-state correlations in the HNC, which is chiefly responsible for the discrepancy between theory and experiment. As shown in the next section, the results of the freezing calculation in the Rogers-Young approximation are much better than those calculated using the HNC theory.

More elaborate schemes for a systematic improvement of our approximations can be devised. Some of the approximations we have tried are

$$C_s^n(\rho) = C_s^0(\rho)\,\delta_{n,0} + C_s^1(\rho)\,\delta_{n,1}, \tag{3.12}$$

which corresponds to improving the single-layer ansatz to include the (presumably most important) off-layer correlations. Another approximation is

$$C_s^n(\rho) = C_s^0(\rho)\,\delta_{n,0} + \exp[-\ell^{-1}(n-1)d] C_s^1(\rho)[1-\delta_{n,0}]. \tag{3.13}$$

Here ℓ is a quantity with the dimensions of length which governs the decay of off-layer correlations, and $C_s^1(\rho)$ is the short-ranged part of $C^1(\rho)$. This corresponds to the assumption that off-layer correlations with $n>1$ are related to off-layer correlations with $n=1$, through a simple exponential prefactor. It is necessary to solve self-consistently for the variable ℓ and for the functions $C_s^0(\rho)$ and $C_s^1(\rho)$. This is done by solving the HNC equations with $n=0$, 1, and 2, and obtaining these parameters and functions self-consistently.

Both these approximations yield results very close to the original scheme of calculation, indicating that the approximation of keeping short-range correlations corresponding to the $n=0$ layer only can be justified over a considerable range of the B-T plane. In the next section, we continue to use this approximation for the off-layer part of the direct correlation function.

IV. CORRELATION FUNCTIONS IN THE ROGERS-YOUNG APPROXIMATION

While the HNC closure is simple and appealing, it is well known that it underestimates correlations in the liquid state, particularly so in the case of long-ranged potentials in two dimensions.[13,43] To illustrate this we plot in Fig. 6 the pair distribution function as calculated in the HNC closure, the Rogers-Young closure (which we discuss in this section) as well as obtained through a Monte Carlo simulation of a simple long-ranged potential [the logarithmic potential in two dimensions or the two-dimensional one-component plasma (2D OCP)]. The data are for a particular value of the dimensionless coupling constant $\Gamma(=100)$ which character-

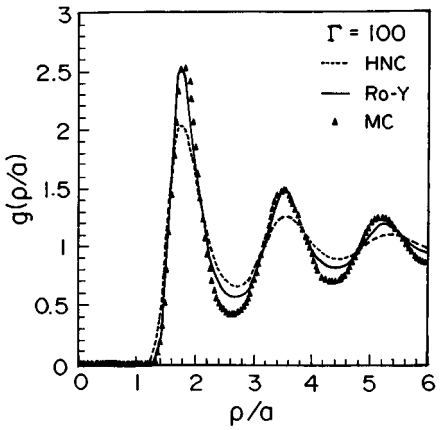

FIG. 6. Comparison of the results for the pair distribution function $g(\rho)$ of the two-dimensional one-component plasma at a coupling constant $\Gamma=100$, obtained from two liquid-state-theories: the hypernetted chain (HNC) approximation (dashed line) and the Rogers-Young approximation (solid line) as well as a Monte Carlo simulation (triangles).

izes the strength of the interaction. Note the considerable discrepancy between the Monte Carlo data as shown in the figure and the results of the HNC closure. As can be seen from Fig. 6, the HNC closure systematically underestimates the structure of the liquid.

This discrepancy may be remedied in one of several ways. Other closure relations exist [all of which correspond to making specific approximations for the bridge function $B(r)$], which are more or less succcessful. The most important of these closures is the Percus-Yevick (PY) closure.[50] In this closure scheme the Bridge function is chosen so that the term involving $Y(r)$ in the exponential can be expanded to yield

$$C(r)=\exp[-\beta V(r)][1+Y(r)]-1-Y(r). \tag{4.1}$$

It is known that the PY closure approximates the correlation functions better at short distances, while the HNC approximation is better at long distances.

The use of hybrid closures (which incorporate some features of HNC and PY) has become increasingly common in recent years. The hybrid closures introduce a (sometimes more than one) parameter such that the relation for $C(r)$ interpolates between a HNC type of closure at long distances and a PY closure at short distances. This parameter is fixed by demanding thermodynamic consistency between compressibility and virial equations of state. The Rogers-Young approximation[40] is one such hybrid closure which takes the form

$$C(r)=\exp[-\beta V(r)]\left[1+\frac{\exp[f(r)Y(r)]-1}{f(r)}\right]-1-Y(r), \tag{4.2}$$

where $f(r)=[1-\exp(-\alpha r)]^m$ is a ''mixing function'' which governs the crossover from a PY type of closure to a HNC type of closure. The parameter α and the exponent m are fixed by demanding thermodynamic consistency. Typically, such thermodynamically consistent liquid-state theories yield results in far better agreement with simulation data than either the PY or the HNC closures separately.

In this section, we describe calculations similar to that of the previous section except that we now employ a Rogers-Young closure to calculate liquid-state properties. The essential approximation we make is the following. From our discussion of the intervortex potential, we derived the asymptotic behavior of the in-plane vortex-vortex interaction to be repulsive and logarithmic in the in-plane separation. This interaction is the same as that in the two-dimensional one-component plasma. This interaction is dominant over much of the phase diagram — for example, at high fields, where the problem becomes essentially two dimensional and freezing of the vortex lattice is driven by nearly independent freezing transitions in each layer, this approximation is very close to reality. We thus expect that treating this part of the interaction more accurately would lead to a better description of the properties of the liquid-state. In the calculations described in this section, we *assume* that the Rogers-Young parameters [the ''mixing length'' α and the exponent m for the in-plane $(n=0)$ equation] are the same as those calculated for the two-dimensional one-component plasma at the appropriate coupling value. We calculate these parameters for the case of the 2D OCP (Refs. 51 and 52) by making use of a exact thermodynamic consistency condition satisfied by the 2D OCP. It reads

$$\frac{\beta P}{\rho_A}=1-\frac{\Gamma}{4}, \tag{4.3}$$

where ρ_A is the areal density, P is the pressure, and Γ is the dimensionless coupling constant that enters the definition of the potential.[53] On the other hand, the regular part of the Fourier space direct correlation function (with the divergent part subtracted out) obeys

$$\lim_{k\to 0}[C(k)+\beta V(k)]=\frac{\delta(\beta P)}{\delta\rho_A}. \tag{4.4}$$

This implies

$$\lim_{k\to 0}[C(k)+\beta V(k)]=\frac{\Gamma}{4}. \tag{4.5}$$

In the usual HNC procedure, this relation is *not* obeyed.

We now describe briefly the details of our numerical procedures. The interaction potential for the 2D OCP is

$$\beta V(\rho)=-\Gamma\ln\frac{\rho}{L}, \tag{4.6}$$

where Γ is a dimensionless coupling constant which characterizes the interaction and L is a scaling length which can be chosen arbitrarily. The Rogers-Young parameters which satisfy this thermodynamic consistency condition for the 2D OCP are plotted in Fig. 7. We scale the potential [Eq. (4.6)] by subtracting a constant term in order that it becomes zero at the upper cutoff length $R_{\max}$. The Rogers-Young parameters plotted here are calculated for a cutoff of 20. We solve the Rogers-Young equation for the 2D OCP using a method similiar to the one described in Sec. III. We then calculate the Rogers-Young parameters by extrapolating the regular

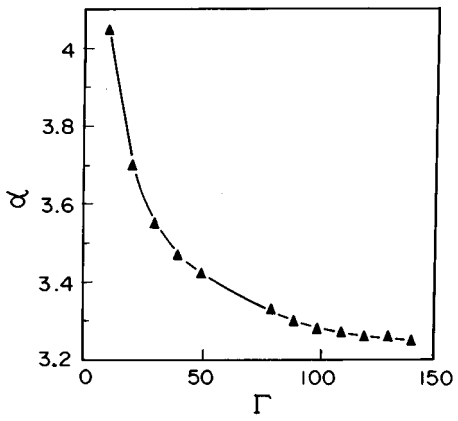

FIG. 7. Dependence of the Rogers-Young parameter α (see text) at thermodynamic consistency on the dimensionless coupling constant Γ for the two-dimensional one-component plasma.

part of the direct correlation function, obtained after converging to self-consistent solutions of the Rogers-Young and Ornstein-Zernike equations, to zero wave vector. The Rogers-Young parameters α and m are varied till thermodynamic consistency [Eq. (4.5)] is achieved. Although for short-range (but power law) potentials in three dimensions the Rogers-Young parameters are found to be approximately constant,[40] such a universality does not seem to hold in the two-dimensional one-component plasma as can be seen from Fig. 7 (such a situation also obtains in the three-dimensional one-component plasma). Our best results are obtained with $m=2$. For large values of Γ, the Rogers-Young parameter α is found to become nearly independent of Γ.

We have also simulated the 2D OCP by Monte Carlo methods, in order to be able to compare our liquid-state results directly with simulations. Because the interaction is long ranged, Ewald summation techniques are required in order to handle the long-range component of the potential correctly. For a system of N particles confined to a rectangle of dimensions $l_x, l_y (A=l_x l_y)$ with periodic boundary conditions, the total interaction energy can be written as[52]

$$E=\frac{e^2}{4}\sum_n \sum_{i=1}^{N} \sum_{j=1}^{N\star} E_1[\alpha_0^2(\mathbf{r}_{ij}+\mathbf{n})^2] + \frac{e^2}{4\pi A}\sum_{k\neq(0,0)} \frac{\exp(-\pi^2\mathbf{k}^2/\alpha_0^2)}{\mathbf{k}^2}\rho_{\mathbf{k}}\rho_{-\mathbf{k}} + \frac{Ne^2}{4}[C+\ln(\alpha_0^2 A)] - \frac{N^2e^2\pi}{4\alpha_0^2 A} \tag{4.7}$$

where E_1 denotes the exponential integral $(E_1(z)=\int_z^\infty [\exp(-t)/t]dt)$, and the Fourier component $\rho_{\mathbf{k}}$ of wave vector $\mathbf{k}=(k_x/l_x, k_y/l_y)$ is given by $\rho_{\mathbf{k}}=\Sigma_i^N \exp(2\pi i\vec{k}\cdot\vec{r}_i)$. C is the Euler constant $(=0.5772)$ and α_0 is a free parameter which can be adjusted to improve the convergence of the series defined above. The sum over $\mathbf{n}$ is over the set of lattice vectors $(n_x l_x, n_y l_y)$. The star on the first summation signifies that the term $i=j$ is to be excluded if $\mathbf{n}=0$. The adjustable length scale L in Eq. (4.6) is taken to be the mean interparticle spacing or the ''ion circle radius'' defined through $a=(\pi\rho_A)^{-1/2}$.

We have simulated this potential of interaction in two dimensions for up to 144 particles, using a standard Monte Carlo algorithm in order to check the quality of our results in the Rogers-Young approximation for the 2D OCP. The interaction potential was tabulated on a grid of size 256×256 and we used linear interpolation to calculate the potential for values of the interparticle separation in between grid points. Typically 2×10^4 Monte Carlo steps (MCS) were performed for extracting thermodynamic and structural quantities after equilibration of a configuration at a particular value of the coupling constant Γ. The program was checked by comparing our results for the excess internal energy and structural data with the results of de Leeuw and Perram who performed a molecular dynamics simulation for the same potential.[52]

Figure 6 displays our results for the pair distribution function in the Rogers-Young approximation and the HNC approximation and also shows the results of the Monte Carlo simulation at $\Gamma=100$. Note the considerable improvement over the ''bare'' HNC theory. While the peaks in the Monte Carlo data are well represented in the Rogers-Young approximation, the troughs are underestimated. This underestimation implies that the structure factor will not be rendered correctly in relation to the Monte Carlo results.

We now rewrite the Rogers-Young closure, so as to ensure that only short-ranged functions are iterated over. Defining short- and long-ranged parts of the correlation function $C^n(\rho)$ and the function $Y^n(\rho)$ as in the previous section we can write

$$C_s^0(\rho)=\exp[-\beta V(\rho,n=0)] \times\left[1+\frac{\exp\{f(r)[Y_s^0(\rho)+\beta V(\rho,n=0)]\}-1}{f(r)}\right] -1-Y_s^0(\rho), \tag{4.8}$$

where $f(r)=[1-\exp(-\alpha r)]^m$ and the symbols have the same meanings as earlier. It is easy to see that the two limits (HNC and PY) are recovered in the appropriate limits.

Our results for the flux-lattice problem follow from essentially the same calculational procedure as before with the difference that we now use Eq. (4.8) to define the short-ranged part of the direct correlation function with $n=0$. The appropriate values of the Rogers-Young parameters are taken to be the same as those for the 2D OCP, at the appropriate coupling constant. Note the factor of 2π that arises in the definition of the coupling constant in the 2D OCP in relation to the coupling constant Γ for the vortex-vortex interaction.

Our results for correlation functions in the liquid-state are shown in Figs. 8–10. In Fig. 8 we show the pair distribution function $g(\rho,n=0)$ as a function of ρ, calculated in the Rogers-Young approximation, for the temperatures $T=18$ and 20 K at a fixed value of the induction $B=5$ kG. In Fig. 9, we show the off-layer pair distribution function $g(\rho,n=1,4,10)$ calculated in the Rogers-Young approximation, at a fixed value of the induction $B=1.4$ kG and a temperature of 30 K. In Fig. 10, we show $\tilde{C}^2(k_\perp a, k_z=0)$ at a fixed temperature $T=20$ K and induction $B=5$ kG.

In Fig. 11, we plot the correlation length Λ in the c-axis direction, obtained by fitting the decay of the peak in $h(\rho,n)$ at $\rho=0$ to an exponential in the layer index n, i.e.,

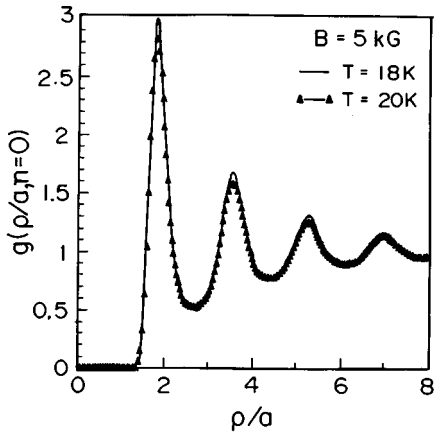

FIG. 8. Pair distribution function $g(\rho,n=0)$ vs ρ calculated in the Rogers-Young approximation for parameter values $B=5$ kG and $T=18$ and 20 K. Note the considerable increase in structure over that seen in the HNC approximation at the same field and temperature.

$$h(\rho=0,n)\sim h(\rho=0,1)\exp(-[n-1]d/\Lambda), \qquad (4.9)$$

with $n\geqslant 2$. This correlation length can be fitted to the form $\Lambda=\Lambda_0+\Lambda_1/B$, with $\Lambda_0/d\simeq 6$. Note that the c-axis correlation length scales inversely with the magnetic induction. For low values of the induction, vortices become increasingly correlated along the c axis, and the mean-field approximation of retaining only on-layer correlations is expected to break down.

A density-functional theory of freezing based on the use of correlation functions from the Rogers-Young closure gives a freezing curve that is shown in Fig. 1 as the sequence of solid squares connected by a solid line. The agreement between theory and experiment is now substantially improved. As in the previous section we have calculated the freezing line in a many-order-parameter approximation. As before, the order parameter jump on freezing is about 0.5 of its zero-temperature value, indicative of a relatively weak first-order transition in contrast to the situtation for isotropic three-dimensional solids where this jump is typically larger than 90%. The value of the Lindemann parameter C_L remains at 0.2.

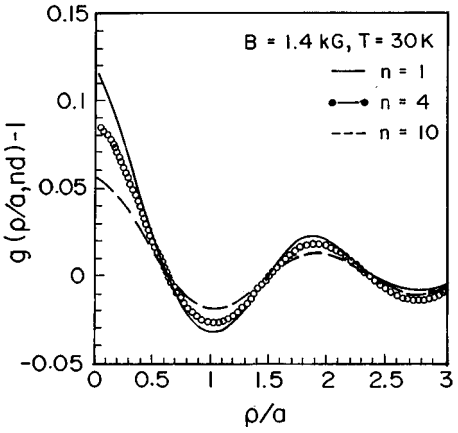

FIG. 9. Off-layer pair distribution function $g(\rho,n)$ vs ρ for $n=1,\ 4,\ 10$, calculated in the Rogers-Young approximation for parameter values $T=30$ K and $B=1.4$ kG.

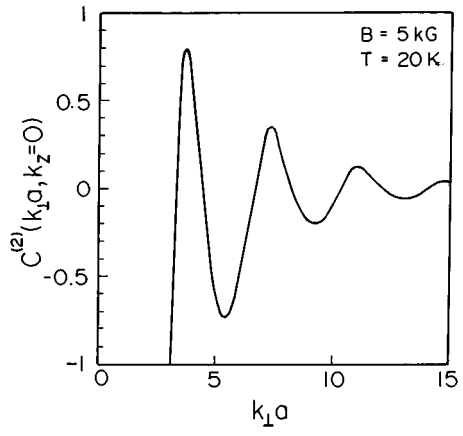

FIG. 10. $\tilde{C}^{(2)}(k_\perp,k_z=0)$ calculated in the Rogers-Young approximation, vs $k_\perp$ for $B=5$ kG and $T=20$ K.

V. CORRELATION FUNCTIONS OF THE LOCAL MAGNETIC INDUCTION

Experiments such as neutron scattering, in contrast to local probes such as muon spin rotation, probe long-range correlations of the magnetic field. In the lattice phase, long-range order in the positions of the flux lines is signaled by the presence of Bragg peaks in the neutron scattering intensity at wave vectors indexing the periodic lattice arrangement. In this section we apply the liquid-state methods developed in Secs. III–IV to the calculation of neutron scattering intensities in the liquid phase of the vortex system. Our results should be directly applicable to SANS measurements of scattered neutron intensities as a function of wave vector. Our basic results are shown in Fig. 12, where we plot the scattered intensities as a function of wave vector for scattering parallel to the layers.

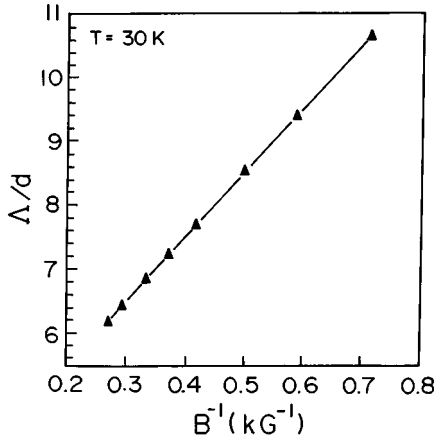

FIG. 11. Dependence of the correlation length Λ for interlayer positional correlations (see text) on the magnetic induction B at $T=30$ K. The results shown were obtained using the Rogers-Young approximation.

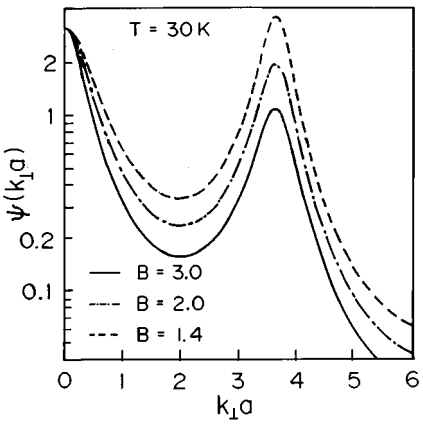

FIG. 12. Magnetic field correlation function $\Psi(k_\perp,0)$ (see text) for $B=3$, 2, 1.4 kG at $T=30$ K. This correlation function is measurable in neutron scattering.

The (dimensionless) magnetic field correlation function is given by the expression

$$\Psi(k_\perp,k_z)=\beta\langle\vec{\mathbf{h}}_{\mathbf{k}}\cdot\vec{\mathbf{h}}_{-\mathbf{k}}\rangle/4\pi V, \tag{5.1}$$

where $\vec{h}(\mathbf{r})$ is the microscopic magnetic field and V is the volume of the sample. This correlation function is proportional to the scattered intensity measured in neutron scattering. The angular brackets denote an ensemble average.

The components of the magnetic field for a vortex on layer $n=0$ can be calculated from Eq. (2.5). They are, in Fourier space,

$$B_z=\frac{d\Phi_0}{1+\lambda^2k_\perp^2+\lambda^2k_z^2} \tag{5.2}$$

and

$$\vec{B}_\perp=-\frac{d\Phi_0k_z\vec{k}_\perp}{k_\perp^2(1+\lambda^2k_\perp^2+\lambda^2k_z^2)}. \tag{5.3}$$

If k_z is zero (i.e., if there is no momentum transfer perpendicular to the layers), the experimental situation corresponds to scattering parallel to the layers. We then have

$$\Psi(k_\perp,k_z=0)=\frac{\rho_A\Gamma\lambda^2}{(1+\lambda^2k_\perp^2)^2}S(k_\perp,0), \tag{5.4}$$

where $S(\vec{k}_\perp,k_z)$ is the dimensionless structure factor of the vortex liquid.

In Fig. 12 we have plotted $\Psi(k_\perp,0)$ for $B=3$, 2, and 1.4 kG at fixed $T=30$ K. The structure factor of the vortex liquid is calculated in the Rogers-Young closure scheme. Note the dramatic increase in the peak in scattered intensity as the transition is approached. This is a consequence of the structure building up in $S(k_\perp,k_z=0)$, as T is decreased or as B is decreased. The increase of structure in each case has a different origin. As the temperature is decreased at fixed field, the increase in structure occurs for the same reason as in classical fluids. On the other hand, as B is decreased at fixed T, the increase in structure is related to the increasing tendency of pancake vortices on each plane to line up to form vortex lines.

VI. CONCLUSIONS

We have presented a theory of flux-lattice melting in high-T_c superconductors which is in agreement with experiments in that it predicts a weak first-order transition between flux-fluid and flux-solid phases, in the experimental situation where the field is applied perpendicular to the layers in a layered system. The shape of our calculated melting curve is also in good agreement with experiment in that our theory is able to reproduce both the strong temperature dependence seen at low fields as well as the characteristic curvature of the melting line in the B-T plane.

While the qualitative features of the phase diagram are rendered accurately, the theoretically obtained melting line as obtained in the Rogers-Young closure still lies some 5° below the experimental boundary. We believe the reasons for this to be the following. The Rogers-Young closure applied to the 2D OCP underestimates the structure factor. As the value of $S(k_\perp,k_z=0)$ at its first peak is the dominant input to the density-functional theory (given the relative smallness of subsidiary peaks), this underestimation would push the melting curve to lower values. Further underestimation comes from the fact that in both the Rogers-Young and the HNC closures, subsidiary peaks in $S(k_\perp,k_z=0)$ are barely present. As discussed by previous authors,[54] inclusion of the effects of these peaks promotes freezing. It is unclear whether the suppression of higher-order peaks in this calculation is an artifact of the Rogers-Young and HNC procedures. Our second comment involves the a-b plane London penetration depth λ_{ab}. There is still considerable discrepancy in quoted values for this quantity, with estimates ranging from 3800 to 1100 Å. It appears reasonable to take values of λ lying between 1400 and 1800 Å (we have used $\lambda=1500$ Å in this calculation). Smaller values of λ would act to shift the melting curve upwards.

We now briefly discuss the approximations we have made and their consequences. First, our approximation of considering only the electromagnetic part of the vortex-vortex interaction is valid only strictly in the limit where the mass anisotropy γ is infinite. While this condition should not, in practice, be important for compounds such as BSCCO or artificially prepared multilayer systems where the interlayer Josephson coupling can be tuned to as small a value as desired, it should break down for less anisotropic systems such as YBCO where the Josephson coupling cannot be neglected over much of the phase diagram. We would expect, in general, the Josephson interaction to move the freezing line to higher temperatures. Including the effects of the Josephson interaction between the vortices cannot be done in any easy way because the interaction is operative only between vortices which belong to the *same* vortex line. We have experimented with various ''pseudopotential'' forms of this Josephson interaction by replacing it by a short-ranged (to account for the effects of cutting and rejoining of vortex lines), attractive interaction between vortices on layers separated by one layer spacing. Numerically, however, the resulting HNC equations are extremely unstable and we have not

been able to obtain well-converged data in this limit. This remains an outstanding problem.

The presence of quenched disorder, usually in the form of oxygen vacancies, is another aspect that we have not dealt with in this paper. In recent work, we have found that a replica-symmetric liquid-state analysis of correlations coupled with the use of a replica density-functional analysis of the disordered liquid to disordered solid transition indicates that the melting line is shifted only very little by weak-point-like sources of disorder (provided that the field is not too large), indicating that our estimate of the freezing line should be robust even in the presence of quenched disorder.[55] While several analytic arguments exist to say that quenched disorder always destabilizes the crystalline lattice ordering on sufficiently large length scales,[56] it is believed that, provided this length scale is much larger than the correlation length of the fluid on freezing, the remnant of the first-order transition in the pure system should be manifest in a discontinuity in some correlation length describing the extent of short-range order in the liquid and the disordered solid phases. Some evidence for this scenario comes from the recent experiments of Zeldov *et al.*,[11] where a discontinuity in the magnetization due to a first-order melting transition is seen at low fields but becomes immeasurably small at somewhat higher fields.

At lower fields than displayed in the theoretically obtained melting curves (Fig. 1) (in practice, for fields less than about 0.5 kg), our *Ansatz* for the off-layer correlation functions breaks down. This is signaled by the direct correlation function $\rho_A C^{(2)}(k_\perp, k_z = 0)$ crossing 1 at some value of $k_\perp$, signaling an instability. This instability is just the consequence of our simple approximation for the interlayer correlation. This instability remains even in the more detailed approximations mentioned at the end of Sec. III, indicating the need for a new approximation for off-layer correlations at low fields. We have experimented with various *Ansätze* for the correlation functions in this limit but have not been able to obtain numerically stable ones. Such a calculation could shed some light on the occurrence of the predicted reentrant melting transition[30] in the very-low-field limit.

ACKNOWLEDGMENTS

We thank the CSIR and UGC (India) for support, the Supercomputer Education and Research Centre (I.I.Sc, Bangalore) for providing computational facilities, and R. Pandit, S.S. Ghosh, S. Bhattacharya, S. Ramakrishnan, and A. Grover for discussions.

*Present address: Theoretical Physics Group, Tata Institute of Fundamental Research, Homi Bhabba Road, Colaba, Bombay-400-005, India.

†Also at Condensed-Matter Theory Unit, Jawaharlal Nehru Centre for Advanced Scientific Research, Bangalore 560 012, India.

[1] A. A. Abrikosov, Zh. Éksp. Teor. Fiz, **32**, 1442-1452 (1957) [Sov. Phys. JETP **5**, 1174 (1957)].

[2] For a recent review of some theoretical aspects of flux lines in superconductors, see G. Blatter, M. V. Feigel'man, V. B. Geshkenbein, A. I. Larkin, and V. M. Vinokur, Rev. Mod. Phys. **66**, 1125 (1994).

[3] K. A. Muller, M. Takashige, and J. G. Bednorz, Phys. Rev. Lett. **58**, 1143 (1987).

[4] Y. Yeshurun and A. P. Malozemoff, Phys. Rev. Lett. **60**, 2202 (1988).

[5] A. P. Malozemoff *et al.*, Phys. Rev. B **38**, 7203 (1988).

[6] E. H. Brandt, Int. J. Mod. Phys. **B 5**, 3313 (1991).

[7] M. P. A. Fisher, Phys. Rev. Lett. **62**, 1415 (1989).

[8] D. S. Fisher, M. P. A. Fisher, and D. A. Huse, Phys. Rev. B **43**, 130 (1990).

[9] M. C. Marchetti and D. R. Nelson, Phys. Rev. B **41**, 1910 (1990).

[10] H. Safar *et al.*, Phys. Rev. Lett.. **69**, 824 (1992).

[11] E. Zeldov *et al.*, Nature **375**, 373 (1995).

[12] S. Bhattacharya and M.J. Higgins, Phys. Rev. Lett. **70**, 2617 (1993); Phys. Rev. B **49**, 10 005 (1994).

[13] S. Sengupta, C. Dasgupta, H. R. Krishnamurthy, G. I. Menon, and T. V. Ramakrishnan, Phys. Rev. Lett, **67**, 3444 (1991).

[14] While the Josephson interaction is relevant at long distances (set by the Josephson length) and converts the asymptotic logarithmic interaction between vortices belonging to the same vortex line on neighboring planes to a linear one, line cutting and rejoining between the planes introduce a length scale into the problem beyond which two flux lines which are displaced by a substantial amount across neighboring planes can minimize their energy by reconnecting. Line cutting and rejoining are expected to be important at high vortex line densities or equivalently large fields.

[15] N. Nakamura, G. D. Guo, and N. Koshizuka, Phys. Rev. Lett. **71**, 915 (1993).

[16] Experiments performed on samples with intermediate to high levels of disorder show behavior consistent with a glassy phase at low temperatures; i.e., the hysteretic behavior associated with the first-order nature of the transition as measured, for example, in transport experiments at low fields (Ref. 10) or the discontinuity in the local induction in Hall probe experiments (Ref. 11), vanishes. The nature of this low-temperature phase is, however, still not well understood although it has been suggested that the superconductor undergoes a transition to a vortex-glass phase in which barriers to flux-line motion diverge exponentially as an externally applied transport current is reduced to zero.

[17] C. Duran *et al.*, Phys. Rev. B **44**, 7737 (1991).

[18] P. L. Gammel *et al.*, Phys. Rev. Lett **59**, 2592 (1987); Phys. Rev. Lett. **61**, 1666 (1988).

[19] Duran *et al.* (Ref. 17) see two peaks when scanning in temperature at fixed field strength and orientation with respect to the *c* axis and ascribe them to separate transitions involving the decorrelation of vortices on different layers at low temperatures and flux-lattice melting at higher temperatures. The second peak is noticeably broader (and thus more suggestive of a crossover than a sharp phase transition) and also more dispersive in temperature (as a function of the angle between the *c* axis and the field), than the first. In addition, at field orientations very close to the *c*-axis orientation, this second dissipation peak is extremely small. For these reasons as well as for reasons of consistency with other experiments, we find it more convincing to identify the transition at lower temperatures with flux-lattice melting. While it has been pointed out [E. H. Brandt, Phys. Rev. Lett. **68**, 3769 (1992)] that two peaks in dissipation could also

arise purely as a consequence of the slab geometry common to samples in these experiments, we believe that such an interpretation is not consistent with the very little variation in the phase boundary seen in experiments performed on crystals of very different dimensions.

[20] A. Schilling, R. Jin, J. D. Guo, and H. R. Ott, Phys. Rev. Lett. **71**, 1899 (1993).

[21] In recent work using Hall sensor arrays and prism-shaped single-crystal samples of BSCCO (which eliminate the geometrical barriers which contribute to irreversibile magnetic behavior), it has been suggested that the irreversibility line and the melting line are, in fact, distinct, with the former being governed wholly by these barriers in sufficiently pure samples [D. Majer, E. Zeldov, and M. Konczykowski, Phys. Rev. Lett. **75**, 1166 (1995)]. In samples with intermediate levels of disorder, however, it appears likely that these geometrical effects can be neglected in comparison to the effects of bulk pinning. As we have shown (Ref. 55), at reasonable levels of pinning for BSCCO, the remnants of the first-order melting transition in the pure system should survive.

[22] R. Cubbitt *et al.*, Nature **365**, 407 (1993).

[23] S. L. Lee *et al.*, Phys. Rev. Lett. **71**, 3862 (1993); S. L. Lee *et al.*, *ibid.* **75**, 922 (1995).

[24] Evidence for a first-order melting transition came initially from experiments by Safar *et al.* (Ref. 10) on single-crystal YBCO in which the linear response resistance was tracked with very high sensitivity across the transition. The data followed two distinct branches on heating and cooling, indicating hysteresis. Similar transport measurements have been reported by W.K. Kwok *et al.*, Phys. Rev. Lett. **72**, 1092 (1994). These experiments have been criticized in work by Jiang *et al.* [W. Jiang *et al.*, Phys. Rev. Lett. **74**, 1438 (1995)], who argue that the hysteresis can be understood as a nonequilibrium effect induced at finite current densities and has no link to an underlying phase transition.

[25] A. Houghton, R. A. Pelcovits, and A. Sudbø, Phys. Rev. B **40**, 6763 (1989).

[26] L. I. Glazman and A. E. Koshelev, Phys. Rev. B **43**, 2835 (1991).

[27] E. H. Brandt, Phys. Rev. Lett. **63**, 1106 (1989).

[28] H.R. Glyde, L.K. Moleko, and P. Findeisen, Phys. Rev. B **45**, 2409 (1992).

[29] While self-consistent phonon theories are an improvement on the earlier calculations of Houghton *et al.* (Ref. 25) and others which use unrenormalized elastic constants, such calculations by construction must always approach melting from the point of view of a lattice instability and as such do not treat the solid and liquid phases on the same footing. Such an approach is also known to severely overestimate melting temperatures in regular three-dimensional solids. Moreover, the calculations of Glyde *et al.* are restricted to a regime where the flux lines do not tilt much from layer to layer, a restriction that is unlikely to represent the correct physics at high fields where, as argued by several authors (Ref. 9), the transverse wandering of the flux lines is considerable across distances of order the interlayer spacing in the layered cuprates.

[30] D. R. Nelson and H. S. Seung, Phys. Rev. B **39**, 9153 (1989).

[31] This problem has been treated in some detail in work by Feigel'man and collaborators (see Secs. V B 2 in Ref. 2).

[32] I. F. Herbut and Z. Tesanovic, Phys. Rev. Lett. **73**, 484 (1994) [see also Z. Tesanovic and L. Xing, *ibid.* **67**, 2729 (1991)]. Herbut and Tesanovic argue that the approximation of retaining the lowest Landau level only should be valid for fields of order and above 1 T in BSCCO. It is not clear to us, however, that their restatement of the problem constitutes a genuine simplification, as their ''dilute vortex plasma'' is not very much more tractable than the original problem.

[33] D. S. Fisher, Phys. Rev. B **22**, 1190 (1980).

[34] M. V. Feigel'man, V. B. Geshkenbein, and A. I. Larkin, Physica (Amsterdam) **167C**, 177 (1990).

[35] S. Ryu, S. Doniach, G. Deutscher, and A. Kapitulnik, Phys. Rev. Lett. **68**, 710 (1992).

[36] R.E. Hetzel, A. Sudbø, and D.A. Huse, Phys. Rev. Lett. **69**, 518 (1992).

[37] Hetzel *et al.* (Ref. 36) do not monitor changes in structural quantities across this transition and their evidence for the transition comes from a finite-size scaling analysis of the energy. Their assumptions ($\kappa \to \infty$) are strictly valid only for fields close to H_{c2}, where the magnetic induction in the superconductor can be taken to be approximately constant. The role played by the latticization procedure (which can artificially stabilize lattice phases by acting as a periodic pinning potential for the vortices) is also ill understood.

[38] R. Sasik and D. Stroud, Phys. Rev. Lett. **75**, 2582 (1995).

[39] Y.-H. Li and S. Teitel, Phys. Rev. Lett. **67**, 2894 (1991).

[40] F. J. Rogers and D. A. Young, Phys. Rev. A **30**, 999 (1984).

[41] W. E. Lawrence and S. Doniach, in *Proceedings of the Twelfth International Conference on Low Temperature Physics*, edited by E. Kanda (Keigaku, Tokyo, 1971).

[42] L. N. Bulaevskii, M. Ledvij, and V. G. Kogan, Phys. Rev. B **46**, 11 807 (1992).

[43] J.P. Hansen and D. R. Macdonald, *Theory of Simple Liquids*, 2nd ed. (Academic, London, 1986).

[44] T. V. Ramakrishnan and M. Youssouf, Phys. Rev. B **19**, 2775 (1979). See D. W. Oxtoby, in *Liquids, Freezing and the Glass Transition*, edited by J. P. Hansen, D. Levesque, and J. Zinn-Justin (North-Holland, Amsterdam, 1990), for a recent review.

[45] Y. Singh, Phys. Rep. **207**, 351 (1991).

[46] S. Sengupta, Ph.D. thesis, Department of Physics, Indian Institute of Science, Bangalore, 1991.

[47] T. V. Ramakrishnan, Phys. Rev. Lett. **48**, 541 (1982).

[48] M.J. Gillan, Mol. Phys. **38**, 6 (1979); **38**, 1781 (1979).

[49] F. Lado, Phys. Rev. B **17**, 2827 (1978).

[50] J. K. Percus and G. J. Yevick, Phys. Rev. **110**, 1 (1958).

[51] J. M. Caillol, D. Levesque, J. J. Weis, and J. P. Hansen, J. Stat. Phys. **28**, 325 (1982).

[52] S. W. de Leeuw and J. W. Perram, Physica **113A**, 546 (1982).

[53] E. Hauge and P. C. Hemmer, Phys. Norv. **5**, 209 (1971).

[54] P. L. Radloff, B. Bagchi, C. Cerjan, and S. A. Rice, J. Chem. Phys. **81,** 1406 (1984).

[55] G. I. Menon and C. Dasgupta, Phys. Rev. Lett. **73**, 1023 (1994).

[56] A. I. Larkin, Zh. Éksp. Teor. Fiz. **58**, 1466 (1970) [Sov. Phys. JETP **31**, 784 (1970)].